ChemComm

COMMUNICATION

View Article Online
View Journal | View Issue

Cite this: *Chem. Commun.*, 2024, **60**, 6785

Received 10th April 2024,
Accepted 1st June 2024

DOI: 10.1039/d4cc01690d

rsc.li/chemcomm

Reduction of (pddi)Cr reveals redox noninnocence *via* C–C bond formation amidst competing electrophilicity: $[(cpta)CrMe_n]^-$ (n = 0, 1) and $[(pta)Cr]^-$†

Alexander A. D'Arpino,[a] Peter T. Wolczanski,*[a] Samantha N. MacMillan,[a] Thomas R. Cundari[b] and Mihail R. Krumov[a]

Reversible cyclopropane formation is probed as a means of redox noninnocence in diimine/diamide chelates *via* reduction and complex anion formation. Competition from imine attack renders complications in the latter approach, and electrochemical measurements with calculational support provide the rationale.

Redox noninnocence (RNI) is a means of expanding the oxidative addition/reductive elimination capability of metal complexes *via* the shuttling of electrons in and out of peripheral ligands.[1–7] Previously, these laboratories explored the concept of redox noninnocence in (pddi)Cr (pddi^{2-} = [Me_2C{CH=N(1,2-C_6H_4)N(2,6-$^iPr_2C_6H_3$)$_2$}]$^{2-}$)[8] *via* cyclopropane C–C bond formation in the ligand backbone.[9–12] Anticipated nitrosylation products containing (cpta)Cr^m (cpta^n = [2-$Me_2C_3H_2${1,2-*N*(1,2-C_6H_4)N(2,6-$^iPr_2C_6H_3$)$_2$}]$^{4-}$) were unrealized, prompting the design of more direct approaches. Herein are examples of C–C bond-forming RNI with the pddi^n ligand, its reversibility, and competing electrophilicity.

Reduction of maroon (pddi)Cr (**1**) with KC_8 in THF, or THF with 1 equiv. 18-crown-6, provided green [(cpta)Cr][K(18-c-6)(THF)$_2$] (**2c**), or hexamer {[(cpta)Cr][K(THF)$_2$]}$_6$ (**2h**) in 76% or 54% yield, respectively. ^{1}H NMR spectra of **2c** or **2h** in THF-d_8 were the same (**2**, sol'n), except for the appearance of 18-crown-6 in the former, and Evans' method[13] measurements were consistent with an S = 3/2 core (μ(eff) = 3.5(1)μ_B). Scheme 1 illustrates a plausible reduction at the ligand (to **1**(−)) rather than at Cr(II), and that subsequent C–C bond formation concomitant with chromium oxidation leads to **2**. Note that K^0 reduction of **1** causes the formal oxidation of Cr(II) to Cr(III) as both imine carbons are reduced. Ferrocinium oxidation (1 equiv.) of **2** caused the complete reversion to **1** over a day, and revealed the reversibility of cyclopropane C–C bond formation. Oxidation is likely to occur from either arene-diamide moiety, with accompanying C–C bond-breaking.

The [(cpta)Cr] anion in **2c** is separate from the [K(18-c-6)(THF)$_2$] cation, and its metrics are clearly those of a tetraamide. Chromium–nitrogen bonds to the imine in **1** (S = 2) average 2.076(9) Å,[8] while the corresponding amide linkages in **2c** average 1.9401(6) Å, and all of its CrN bond distances are shorter in concert with the change from Cr(II) to Cr(III).[14] The cyclopropane C–N single bond lengths are 1.4316(6) (ave) Å while the related imine distances are 1.289(4) (ave) Å,[15] and the new C–C bond is 1.509(2) Å, a distance whose bond enthalpy is about 101(2) kcal mol^{-1}.[16] Select core distances and angles in **2c** are listed in the caption to Fig. 1 and reflect its S = 3/2 ground state. A partial skeletal view of the hexamer, **2h** is also shown, and its core distances are within 0.002 Å and 1° of those in **2c**, except for those involving N1, whose subtle angular changes with connected atoms are features of the hexamer.

As Scheme 2 illustrates, treatment of (pddi)Cr (**1**) with MeLi in THF induced formal oxidation of Cr(II) to Cr(IV) concomitant with Me anion adduct formation and 2e$^-$ reduction of the

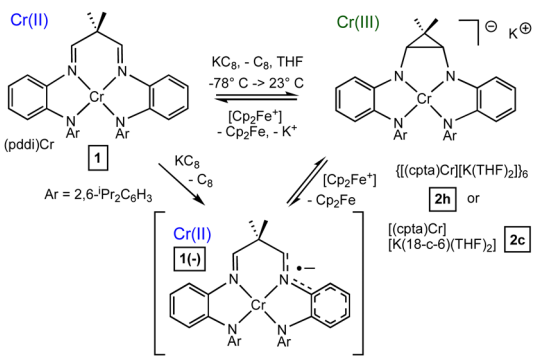

Scheme 1 Reduction of (pddi)Cr (**1**) and oxidation of [(cpta)Cr][K(18-c-6)(THF)$_2$] (**2**) showing reversible cyclopropane C–C bond formation.

[a] *Department of Chemistry and Chemical Biology Baker Laboratory, Cornell University, Ithaca, NY 14853, USA. E-mail: ptw2@cornell.edu*

[b] *Department of Chemistry, CasCam, University of North Texas, Denton, TX 76201, USA*

† Electronic supplementary information (ESI) available. CCDC 2345829–2345833. For ESI and crystallographic data in CIF or other electronic format see DOI: https://doi.org/10.1039/d4cc01690d

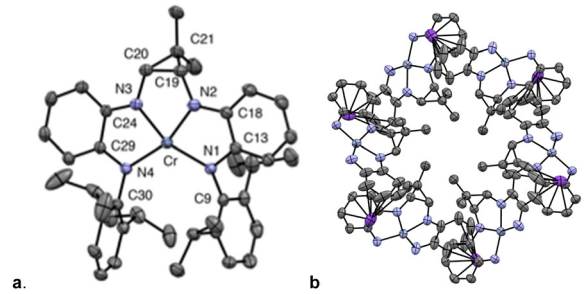

Fig. 1 (a) Molecular view of the [(cpta)Cr] anion of (**2c**). Selected distances (Å) and angles (°): CrN1, 2.0016(12); CrN2, 1.9405(13); CrN3, 1.9396(13); CrN4, 1.9976(12); N1C13, 1.3928(18); N2C18, 1.366(2); N2–C19, 1.4311(19); C19C20, 1.509(2); N3C20, 1.432(2); N3C24, 1.3634(19); N4C29, 1.3864(17); N1CrN2, 80.38(5); N1CrN3, 159.43(5); N1CrN4, 119.49(5); N2CrN3, 80.94(5); N2CrN4, 159.75(5); N3CrN4, 79.91(5); N2C19C20, 110.73(13); N2C19C21, 119.70(15); N3C20C19, 110.57(13); N3C20C21, 120.84(15). (b) K[arene-diamide]$_6$ connectivity of **2h**; THFs and 2,6-^{i}Pr$_2$C$_6$H$_3$ groups removed for clarity.

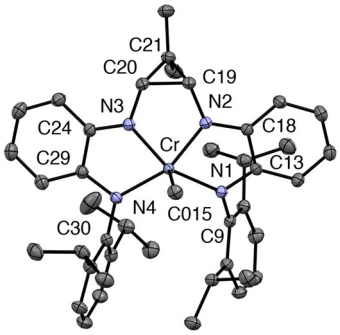

Fig. 2 Molecular view of the [(cpta)CrMe] anion of (**3**). Selected distances (Å) and angles (°): CrN1, 1.9968(12); CrN2 1.9382(12); CrN3 1.9285(13); CrN4, 2.0398(12); CrC015, 2.0766(15); N1C13, 1.3931(18); N2C18, 1.3582(19); N2–C19, 1.4251(18); C19C20, 1.502(2); N3C20, 1.4269(18); N3C24, 1.3618(19); N4C29, 1.3804(19); N1CrN2, 80.35(5); N1CrN3, 150.83(5); N1CrN4, 114.37(5); N2CrN3, 79.81(5); N2CrN4, 157.13(5); N3CrN4, 79.60(5); N1CrC015, 97.16(6); N2CrC015, 92.31(6); N3CrC015, 104.80(6); N4CrC015, 102.50(6); N2C19C20, 109.68(12); N2C19C21, 117.87(12); N3C20C19, 110.46(12); N3C20C21, 119.48(13).

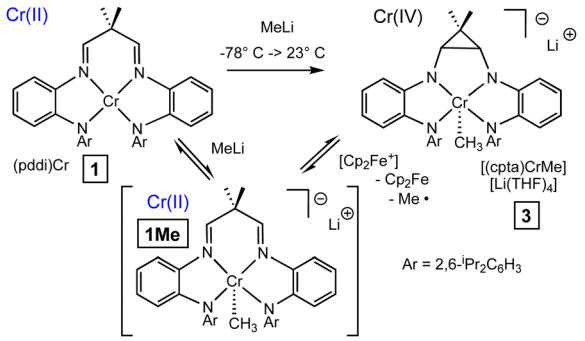

Scheme 2 Reduction of (pddi)Cr (**1**) with MeLi to afford [(cpta)CrMe]-[Li(THF)$_4$] (**3**).

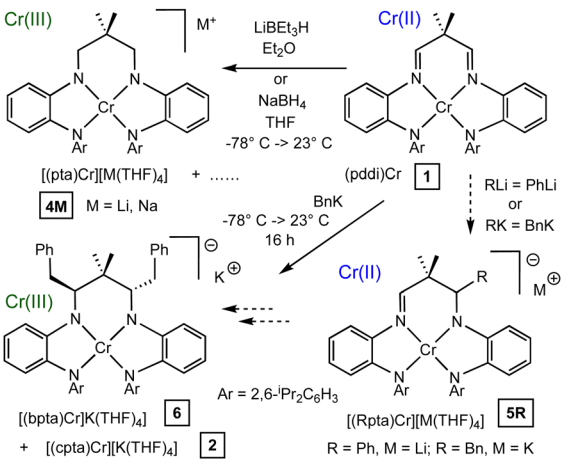

Scheme 3 Hydride and benzyl anion addition to (pddi)Cr (**1**).

chelate. Cyclopropanated product [(cpta)CrMe][Li(THF)$_4$] (**3**) is paramagnetic (S = 1; μ(eff) = 2.7(1)μ_B)[13] and was isolated in 63% yield. It is likely that adduct formation to Cr(II) incurs only a modest electronic change, and the added electron density induces the 2e$^-$ diimine coupling to generate the formal Cr(IV) tetraamide ^{c}Pr-containing chelate, cpta.

With an Addison parameter of τ = 0.11,[17] the [(cpta)CrMe] anion of **3** is clearly pseudo square pyramidal, with core N–Cr–C angles varying from 92.31(6)° to 104.80(6)°. The average deviation of N(amide)Cr distances between **2** and **3** is 0.006 Å, with the greatest 0.0422 Å, hence the formal oxidation state change is not metrically evident.[18] Pertinent bond distances and angles are listed in the Fig. 2 caption.

Many reagents that can be construed as nucleophiles were unreactive with (pddi)Cr (**1**), *e.g.* PMe$_3$ or N_3^-, and others manifested alternative paths to adduct formation. Evidence of 1e$^-$ reduction was observed for $NaNH_2$, and the pddi proved susceptible to attack by hydride and other alkyl anion sources. As Scheme 3 reveals, addition to the electrophilic imines was observed with $LiBEt_3H$ or $NaBH_4$ to afford tetraamide [(pta)Cr][M(THF)$_4$] (**4M**, M = Li, Na) in 68% or 46% yield. Unidentifiable disproportionation product(s) are likely to balance the double hydride addition to **1**.

The molecular view of the [(pta)Cr] anion of **4Li** is pseudo square planar (Fig. 3), with core Cr–N distances consistent with an S = 3/2 (μ(eff) = 3.9(1)μ_B)[13] tetraamide, and within 0.03 Å of those of **2** and **3**. Carbon–nitrogen bond lengths of 1.458(2) and 1.457(2) Å in the propyl ligand backbone are clearly those of single bonds,[15] and related angles of the methylenes are those of strained sp^3-carbons: 115.81(14)° and 113.32(14)°.

In concert with hydride addition, exposure of (pddi)Cr (**1**) to BnK afforded the analogous double addition product [(bpta)Cr][K(THF)$_4$] (**6**), and in this case, crystallization with 18-c-6 present afforded a 1 : 1 mixture of **6** : **2**, which eluded separation. The reaction of **1** and PhLi revealed Ph addition to one imine, consistent with the triamide [(Rpta)Cr][M(THF)$_4$] (**5R**; R = Ph, M = Li; R = Bn, M = K), according to a partial X-ray structure determination that provided the connectivity. A related benzyl

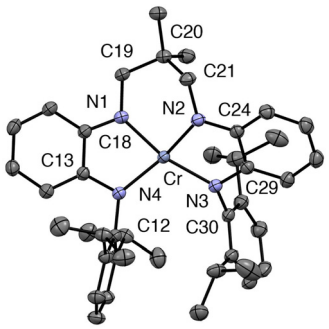

Fig. 3 Molecular view of the [(pta)Cr] anion of (**4Li**). Selected distances (Å) and angles (°): CrN1, 1.9594(14); CrN2, 1.9663(14); CrN3, 1.9928(14); CrN4, 2.0089(14); N4C13, 1.391(2); N1C18, 1.369(2); N1–C19, 1.458(2); N2C21, 1.457(2); N2C24, 1.374(2); N3C29, 1.388(2); N1CrN2, 92.39(6); N1CrN3, 162.74(6); N1CrN4, 81.14(6); N2CrN3, 80.72(6); N2CrN4, 164.57(6); N3CrN4, 109.19(6); N1C19C20, 115.81(14); N2C21C20, 113.32(14).

Cr(II) complex (**5Bn**) is a plausible intermediate that can transfer an electron to (pddi)Cr (**1**) to afford **2**. The resulting neutral Cr(III) benzylated complex is likely susceptible to attack by a second BnK to provide **6**.

Fig. 4 illustrates the dibenzylated anion of [(bpta)Cr][K(18-c-6)(THF)$_2$] (**6**) that cocrystallized with **2c**. Chromium–nitrogen bond distances listed in the caption are consistent with amide linkages, and the backbone CC- and CN-distances possess C(sp^3)–C(sp^3), and the N–C(sp^3) values.[15] The pseudo square-planar coordination manifests greater distortion ($\Sigma\ \angle$NCrN = 375.9°) than **1** (360.8°),[8] **2c** (360.7°), and **4** (362.9°), presumably due to the tetraamide core in combination with the added sterics of the anti-arrangement of the benzylated backbone.

Free energy calculations pertinent to Schemes 1 and 2 are given in Scheme 4. While reduction of (pddi)Cr (**1**) to [(cpta)Cr]K(THF)$_n$ (**2**) was suggested to occur *via* a 1e$^-$-reduced intermediate (**1**(−)), it is surprising that thermal formation of the neutral (cpta)Cr (**1CC**) complex is only 11.8 kcal mol^{-1} endoergic, providing an alternative path, one that is common to Scheme 2. Adduct formation of MeLi and **1** to **1Me** is exoergic by −7.2 kcal mol^{-1}, and the ensuing CC-bond formation to [(cpta)CrMe][Li(THF)$_n$] (**3**) is also favorable by

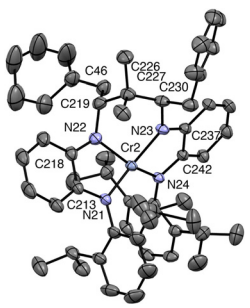

Fig. 4 Molecular view of the [(bpta)Cr] anion of (**6**). Selected distances (Å) and angles (°): Cr2N21, 1.9786(15); Cr2N22, 1.9345(17); Cr2N23 1.9643(15); Cr2N24, 1.9673(15); N22C219, 1.463(3); N23C227, 1.469(2); C219C226, 1.561(3); C219C46, 1.541(3); C226C227, 1.556(3); C227C230, 1.562(3); N21Cr2N22, 81.62(7); N21Cr2N23, 149.04(7); N21Cr2N24, 120.22(6); N22Cr2N23, 92.34(7); N22Cr2N24, 144.00(7); N23Cr2N24, 81.66(6).

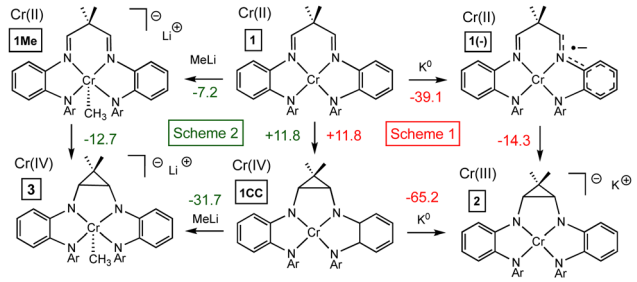

Scheme 4 Calculated free energies (kcal mol^{-1}) of paths pertinent to Scheme 1 (red) and 2 (green) relative to (pddi)Cr (**1**) at 0.0 kcal mol^{-1}.

−12.7 kcal mol^{-1}. While the likely path, barriers to even these simple paths involving charged species are difficult to assess, and while formation of **1CC** is endoergic by +11.8 kcal mol^{-1}, the adduct might form *via* an empty d_{z^2} orbital on the Cr(IV) species.[19]

The cyclic voltammogram of (pddi)Cr (**1**) in Fig. 5 shows a reduction at −2.50 V (rel. to Fc/Fc$^+$), followed by a second at −2.76 V. An oxidation wave at −2.53 V and another at much more positive potential (−0.99 V) are also observed. If the potential is cycled immediately after the first reduction wave, only the oxidation at −0.99 V is observed, consistent with reduction to [(pddi)Cr]$^-$ (**1**(−)), followed by rapid CC bond formation to **2**, and oxidation back to **1**, with ΔE_p = 1.51 V. The second reduction and corresponding oxidation likely correspond to a reversible [(cpta)Cr]$^-$ (**2**) to [(cpta)Cr]$^{2-}$ couple.

Molecular orbitals corresponding to (pddi)Cr (**1**) and [(cpta)Cr][K(THF)$_n$] (**2**) reveal the consequences of low symmetry and unpaired spins (Fig. 6); virtually all are admixtures of ligand and Cr(3d). A 1e$^-$ reduction of **1** is likely to be in the β-LUMO (Lπ*, −1.35 eV) resulting in an S = 3/2 configuration due to antiferromagnetic (AF) coupling. The ensuing formation of **2** *via* C–C bond formation is spin-allowed, and likely to occur immediately to attenuate electron density near and at the Cr. This is supported by the calculated favorable free energy (−14.3 kcal mol^{-1}, Scheme 4) for **1**(**1**−) → **2**, and the MO of **2**, which manifests a low-lying α-LUMO at −1.39 eV. It can accept an

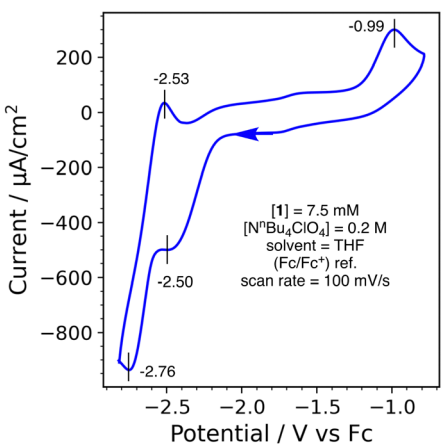

Fig. 5 Cyclic voltammogram of (pddi)Cr (**1**).

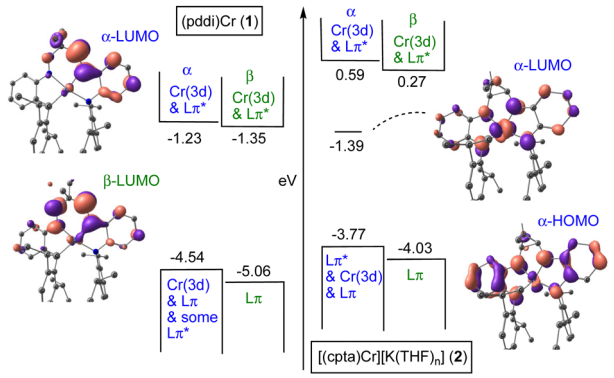

Fig. 6 Respective relative α (blue) and β (green) molecular orbitals of (pddi)Cr (**1**) and [(cpta)Cr][K(THF)$_n$] (**2**); details are found in the ESI.†

electron consistent with the aforementioned reversible reduction at −2.76 V. The low-lying β-LUMO (Lπ*) MO of **1** is also a site that invites nucleophilic attack, as observed for the hydride, Ph(−) and Bn(−) chemistry in Scheme 3.

Formation of [(cpta)CrMe][Li(THF)$_n$] (**3**) is less well rationalized. Empty Cr(3d) orbitals and ligand (Lπ*) orbitals of (pddi)Cr (**1**) are positioned similarly according to energy, but d_{z2} is half-occupied, affording some e^-–e^- repulsion upon an axial nucleophilic attack. It is intriguing that cyclopropane formation (**1** → **1CC**, Scheme 4) is calculated to by only 11.8 kcal mol^{-1} endoergic, perhaps suggesting a means of allowing attack at an empty d_{z2} orbital. MOs of **3** are admixed to the extent that identifying α- and β-orbitals as primarily Cr(d)- or ligand-based is not appropriate. Consequently, while formal oxidation states (FOSs) are used to classify these complexes, the similar structural metrics of **1**, **2c**, **3**, **4Li**, and **6** show that the variance upon oxidation is modest.[18] It is clear that storing electrons in a C–C bond can be incorporated into a ligand for RNI applications.

All synthetic and most spectroscopic work was conducted by AAD; MRK performed the cyclic voltammetry; TRC is responsible for calculations, and SNM is the crystallographer. Conception of the project and management is the purview of PTW.

Support from the National Science Foundation (PTW, CHE-1953884; UNT, OAC-2117247), the Dept. of Energy (TRC, DE-FG-03ER15387), and Cornell University is gratefully acknowledged.

Conflicts of interest

There are no conflicts to declare.

Notes and references

1 C. K. Jorgensen, *Helv. Chim. Acta*, 1967, **50**(supp. 1), 131–146.
2 C. G. Pierpont, *Coord. Chem. Rev.*, 2001, **255**, 837–860.
3 R. Eisenberg and H. B. Gray, *Inorg. Chem.*, 2011, **50**, 9741–9751.
4 (*a*) C. Römelt, T. Weyermüller and K. Wieghardt, *Coord. Chem. Rev.*, 2019, **380**, 287–317; (*b*) K. Ray, T. Petrenko, K. Wieghardt and F. Neese, *Dalton Trans.*, 2007, 1552–1556.
5 C. C. Lu, E. Bill, T. Weyermüller, E. Bothe and K. Wieghardt, *J. Am. Chem. Soc.*, 2008, **130**, 3181–3197.
6 (*a*) V. Lyaskovskyy and B. De Bruin, *ACS Catal.*, 2012, **2**, 270–279; (*b*) N. P. van Leest, R. F. Epping, K. M. van Vliet, M. Lankelma, E. J. van den Heuvel, N. Heijbrink, R. Broersen and B. de Bruin, *Adv. Organomet. Chem.*, 2018, **70**, 71–180.
7 R. F. Munha, R. A. Zarkesh and A. F. Heyduk, *Dalton Trans.*, 2013, **42**, 3751–3766.
8 A. A. D'Arpino, T. R. Cundari, P. T. Wolczanski and S. N. MacMillan, *Organometallics*, 2023, **42**, 2747–2761.
9 E. B. Hulley, S. P. Heins, P. T. Wolczanski, K. M. Lancaster and E. B. Lobkovsky, *Polyhedron*, 2019, **159**, 225–233.
10 (*a*) F. Fransceschi, E. Solari, R. Scopelliti and C. Floriani, *Angew. Chem., Int. Ed.*, 2000, **39**, 1685–1687; (*b*) R. Crescenzi, E. Solari, C. Floriani, A. Chiesi-Villa and C. Rizzoli, *J. Am. Chem. Soc.*, 1999, **121**, 1695–1706; (*c*) E. Gallo, E. Solari, N. Re, C. Floriani, A. Chiesi-Villa and C. Rizzoli, *J. Am. Chem. Soc.*, 1997, **119**, 5144–5154; (*d*) S. Gambarotta, C. Floriani, A. Chiesi-Villa and C. Guastini, *J. Chem. Soc., Chem. Commun.*, 1982, 756–758.
11 (*a*) J. Bachmann and D. G. Nocera, *J. Am. Chem. Soc.*, 2005, **127**, 4730–4743; J. Bachmann and D. G. Nocera, *J. Am. Chem. Soc.*, 2004, **126**, 2829–2837; (*b*) J. Bachmann, J. M. Hodgkiss, E. R. Young and D. G. Nocera, *Inorg. Chem.*, 2007, **46**, 607–609.
12 D. Bhattacharya, S. Dey, S. Maji, K. Pal and S. Sarkar, *Inorg. Chem.*, 2005, **44**, 7699–7701.
13 (*a*) D. F. Evans, *J. Chem. Soc.*, 1959, 2003–2005; (*b*) E. M. Schubert, *J. Chem. Educ.*, 1992, **69**, 62.
14 A. G. Orpen, L. Brammer, F. H. Allen, O. Kennard, D. G. Watson and R. Taylor, *J. Chem. Soc., Dalton Trans.*, 1989, S1–S83.
15 F. H. Allen, O. Kennard, D. G. Watson, L. Brammer, A. G. Orpen and R. Taylor, *J. Chem. Soc., Perkin Trans. 2*, 1987, S1–S19.
16 A. A. Zavitsas, *J. Phys. Chem. A*, 2003, **107**, 897–898.
17 A. W. Addison, N. T. Rao, J. Reedijk, J. van Rijn and G. C. Verschoor, *J. Chem. Soc., Dalton Trans.*, 1984, 1349–1356.
18 P. T. Wolczanski, *Organometallics*, 2017, **36**, 622–631.
19 S. P. Heins, W. D. Morris, T. R. Cundari, S. N. MacMillan, E. B. Lobkovsky, N. M. Livezey and P. T. Wolczanski, *Organometallics*, 2018, **37**, 3488–3501.

